Title
RELATIVE THRESHOLDS FOR PRODUCTION OF IODINE ISOTOPES FROM FUSION AND TRANSFER-INDUCED FISSION REACTIONS

Author
De Saint-Simon, M.

Publication Date
1977-11-01

Submitted to Physical Review C

LBL-7114
Preprint

RELATIVE THRESHOLDS FOR PRODUCTION OF IODINE ISOTOPES FROM FUSION AND TRANSFER-INDUCED FISSION REACTIONS

M. de Saint-Simon, R. J. Otto, and
G. T. Seaborg

November 1977

Prepared for the U. S. Department of Energy
under Contract W-7405-ENG-48

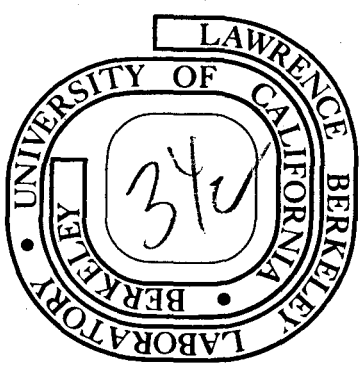

DISCLAIMER

RELATIVE THRESHOLDS FOR PRODUCTION OF IODINE ISOTOPES FROM FUSION AND TRANSFER-INDUCED FISSION REACTIONS

M. de Saint-Simon

Laboratorie Rene Bernas - BP1 - 91406 Orsay - France

R. J. Otto and G. T. Seaborg

Nuclear Science Division
Lawrence Berkeley Laboratory
University of California
Berkeley, California 94720

ABSTRACT

The reaction of ^{40}Ar ions with energies from 212 to 340 MeV impinging on a thick ^{238}U target has been studied using radiochemical methods. The formation cross sections of iodine isotopes were measured and converted to independent yields from which isotopic distributions were derived. The observed shape of the iodine distributions is attributed to entrance channel mechanisms: quasielastic transfer (QET), deep inelastic transfer (DIT) and complete fusion (CF), each followed by fission. The width and shape of the complete fusion component are found to be consistent with the statistical model for fission and the "overlaid-ALICE" code for the fragment deexcitation. The threshold for production of iodine isotopes by the CF reaction is found to be at least 15 MeV higher in energy than the barrier for the production of iodine isotopes by the QET reaction. These barriers are compared with theoretical predictions.

[NUCLEAR REACTIONS, FISSION $^{238}U(^{40}Ar,X)$ I, E_{lab} = 212, 226, 240, 250, 270, 290, 340 MeV; measured σ (iodine isotopes); deduced σ (independent yield iodine isotopes), relative thresholds for complete fusion and quasielastic transfer.]

I. INTRODUCTION

The system $^{40}Ar + ^{238}U$ has been studied by many authors because it deals with a medium mass heavy ion and a heavy target. In the entrance channel of such a system, several different mechanisms are competing: complete fusion (CF), quasielastic transfer (QET) (inelastic scattering and few nucleon transfer) and deep inelastic transfer (DIT), in each of which the heavy product may undergo fission. In this case, the compound nucleus $^{278}(110)$ has a fission barrier equal to zero so that the probability of first chance fission, based on the classical model of the fission process, is expected to be close to one. These particular entrance channel processes are of interest in understanding the dynamics of heavy-ion reactions.

Among the many studies of this system, only a few have concentrated on the reaction cross sections for the above reaction mechanisms, and these studies[1-7] generally were done at only one value of the projectile energy.

In order to investigate the behavior of the QET, DIT and CF processes as a function of the bombarding energy we used a method sensitive to all competing reaction channels: the radiochemical measurement of the production cross sections of iodine isotopes with a thick uranium target. These experiments were carried out at seven energies of the argon ion beam, ranging from the Coulomb barrier to 340 MeV. This method allows us to determine the isotopic distribution of iodine after making growth and decay and recoil loss corrections to obtain the independent yields.

The final isotopic distributions reveal the occurrence of the three mechanisms. The shape of the isotopic distributions is found to be in agreement with that expected for the quasielastic transfer, deep inelastic transfer and complete fusion components after taking into account the energy spread due to the thickness of the target. Furthermore the data show that the complete fusion process has a higher energy threshold than the other processes.

In Sec. II the experimental method is described and the results are presented.

In Sec. III the data are analyzed using the statistical model of fission to estimate the width and center of the iodine isotopic distribution from the complete fusion-fission process. The "overlaid-ALICE" code is used to determine the particle evaporation process in the deexcitation of the fission fragments.

In Sec. IV a comparison is made of the relative thresholds for the production of iodine isotopes in the identified reaction mechanisms (QET, DIT, CF). An interpretation of the results is given by assuming 1) a relatively higher threshold for complete fusion than for the QET and DIT reactions, or 2) asymmetric fission of the compound nucleus near the reaction barrier. Arguments in favor of the first interpretation are given and a comparison with theoretical predictions for the higher complete fusion threshold is made. The paper is summarized in Sec. V.

II. EXPERIMENTAL

The uranium targets used in these experiments consisted of 30 mg/cm^2 depleted ^{238}U metal that had been sputtered onto a 5-mm aluminum backing plate. A thin layer of Al (50-100 μg/cm^2) was then evaporated onto the surface of the uranium to prevent oxidation. The targets were mounted inside the Faraday cup. A tantalum collimator with a 6-mm diam aperture was used ahead of the target. Several tests were carried out to assure that accurate beam intensity measurements could be made with the target holder system used.

The beam energy was measured before and after each run and no significant energy changes were noted. The energies were measured with a gold surface barrier detector placed directly in the beam path. The surface barrier detector was calibrated using a linear pulsar extrapolation of a calibration of the detector using the known energies of the ^{212}Po and ^{212}Bi alpha particle emitters. The pulse height defect is known to be 2 to 3 MeV for ^{40}Ar in this energy range.[8] The corrections for energy loss in the Al cover layer corresponded to 0.9 to 1.2 MeV at most and this correction tends to partially cancel the pulse height defect energy correction of the crystal. Corrections to the measured beam energy corresponded to adding 1.0 to 1.5 MeV to the measured energies, which was less than the uncertainty in the beam energy. Table I summarizes the ^{40}Ar + ^{238}U irradiations. The effective target thicknesses correspond to the range of ^{40}Ar ions from the incident energy to the barrier that was taken to be 200 MeV. The Northcliffe Shilling range tables were used.[9]

Within 10 min of the end of bombardment the targets were prepared for chemical separation of iodine. The Al cover layer was first dissolved from the surface of the uranium using 10 M NaOH solution. The surface was washed with water and a dissolving and distilling chimney was attached to the target. A small amount of carrier solution (100µl) containing HI and HBr was added to the dissolving chimney followed by 100 µl HNO_3 and a small amount of H_2O. The dissolution of the target and evolution of I_2 and Br_2 was carried out by gentle heating. The I_2 and Br_2 gases were caught in a carbon tetrachloride trap. After complete dissolution of the target and partial dissolution of the Al backing plate to insure that all of the fission products were dissolved the I_2 and Br_2 were extracted from the CCl_4 solution using an aqueous solution of SO_2. An AgI/AgBr precipitate was obtained and filtered onto cellulose nitrate filter paper. The precipitate and filter paper were taped to a planchet and placed in front of a Ge(Li) spectrometer.

The chemical yield of the iodine fission products was later determined by neutron activation of ^{127}I to produce ^{128}I activity in the above samples and in a standard prepared at the time of the ^{40}Ar irradiations. These chemical yields are given in Table I.

The Ge(Li) spectrometer system used to obtain the gamma-ray spectra between 90 keV and 2 MeV had a resolution of 2.1 keV for the 1332 keV ^{60}Co gamma ray. The absolute efficiency for the counting geometry used was known to be within 5%. The AgI, AgBr samples were counted for regularly increasing periods, starting approximately 30 min after the end of bombardment and extending to 2 to 3 weeks thereafter.

The gamma-ray spectra were analyzed using the AESl analysis code.[10] The identified peaks were then sorted by energy and arranged so that the decay curve and energy of each of the peaks could be graphically displayed along with a corresponding list of 20 isotopes having gamma rays with the same or nearly the same energy. The final assignment and identification of a nuclide was based on agreement of the energy, half-life and relative abundance of the observed gamma rays. Production cross sections for the identified nuclides were then calculated and the final uncertainty reflects the errors in the half-life fits to the data, the counting efficiency and the chemical yield.

The experimental results are plotted in Fig. 1. These cross sections represent the measured partial cumulative and independent yields. In order to calculate the independent yields from the measured partial cumulative yields, the fractional independent yields of the parent and grandparent, etc. isotopes for each of the iodine isobars must be known. The isotopic mass dispersions for the iodine isotopes appears to be generally double peaked. The explanation[11] that have been put forth for these two peaked distributions is that the neutron excessive products are fission products from quasielastic transfer (QET) induced fission of the U target, and the neutron deficient products and shielded isotopes near the valley of beta stability are products from complete fusion (CF) followed by fission of the compound nucleus. Using this interpretation an iterative procedure was used to calculate the independent yield isotopic distribution of the iodine isotopes based on two gaussian charge dispersions. The known charge distribution

widths and centers[12] for 40 MeV proton induced fission of ^{238}U were used as a model for the QET induced fission and a guassian charge distribution centered near the valley of beta stability was used for the CF induced fission. Although the magnitudes of both distributions were allowed to vary until a best fit was obtained, only in the case of the second, more neutron deficient distribution was the center and width of the guassian allowed to vary.

The final correction to the data was for recoil losses from the face of the target corresponding to fission fragments moving backward in the laboratory reference frame. The recoil loss corrections were calculated separately for the iodine products from fission of the compound nucleus and for fission of uranium-like products in the QET reaction, since these two fission sources have different center-of-mass velocities and total kinetic energies. The center-of-mass velocities of the uranium-like QET products were estimated by calculating the c.m. system velocity at the classical grazing angle for a purely elastic collision. These recoil loss corrections were integrated over the effective target thickness, and the decreasing bombarding energies were taken into account. A recoil range distribution code described by Otto et al.[13] was used to make the recoil loss calculations assuming a $1/\sin\theta$ type angular distribution for the fission fragments from the complete fusion reaction and an isotropic distribution for fission following QET of the uranium-like products.

The numerical values of the final independent yield cross sections are summarized in Table II and the iodine isotopic distributions are plotted in Fig. 2. The main features of these distribution are the

following:

1. They have a two (or three) peaked structure;
2. The centroids of the peaks move very slightly with the projectile energy;
3. The relative height of the two main peaks depends on the projectile energy in agreement with the interpretation that at least two different processes (QET induced fission and CF induced fission) can be correlated with two separate but superimposed iodine fission product distributions.

It should be pointed out that the shapes of the final distributions shown in Fig. 2 are not very sensitive to the shapes of the two guassian charge dispersions assumed for the purpose of growth and decay corrections. This fact, along with a number of measured independent yields, makes the results of Fig. 2 and Table II independent, to a large degree, of the models used for the charge dispersion description.

III. ANALYSIS OF THE ISOTOPIC YIELD DISTRIBUTIONS

A. Quasielastic transfer-fission component

In order to understand the main features of these results, we shall try to analyze the two main peaks of these isotopic yield distributions in two successive steps.

We begin with the now classical ideas that the neutron rich distribution is coming from the fission of target-like nuclei produced by the quasielastic transfer reaction. The neutron deficient distribution is attributed to fission proceeding from the complete fusion process. We shall check these assumptions and look at the trends of the results when the bombarding energy is increasing.

Let us consider the first process. Our results are in good agreement with the analysis done by Kratz et al.[6] for the same reaction at 288 MeV also obtained with a thick target. The neutron rich distribution is well reproduced by a gaussian curve where the independent yield of the isotope of mass A is given by

$$P(A) = \frac{C}{\left(2\pi\sigma_A^2\right)^{1/2}} \exp - \frac{(A - A_p)^2}{2\sigma_A^2} \qquad (1)$$

where A_p is the most probable mass and σ_A^2 the variance describing the width of the distribution, with $A_p = 134.3$ and $\sigma_A^2 = 4.4$. This result corresponds to the low energy fission of target-like nuclei with excitation energy about 15 to 20 MeV.[8,14] Another method is to use the Cs isotopic distribution results obtained by on-line

mass spectrometry for the reaction ^{238}U + (40 MeV)p by Tracy et al.[12] to fix the center and width of the QET induced fission distribution. This measured Cs isotopic distribution was used with success to explain the results obtained for the reaction ^{20}Ne + ^{238}U by Reisdorf et al.[8] for the quasielastic transfer component. In the reaction U + p at 40 MeV, taking prescission evaporation into account, the fissioning nuclei are essentially $^{238-x}Np$ ($x = 2 \pm 1$) at an excitation energy of 20 ± 10 MeV. The Cs isotopic distribution, corrected for the mass shift due to the difference for the Z value between Cs (Z = 55) and I (Z = 53) should be approximately representative for the iodine isotopic distributions from fission following direct reactions of Ar with U at the energies involved in our experiment. In Fig. 2 we have plotted this isotopic distribution (dashed line) along with our experimental points. By adjusting the absolute value of the cross sections for the p + U curve, a good fit is obtained for neutron excessive mass distribution, even though we have no experimental point beyond the mass number 135. The small discrepancies on the left side of the bump are due to the proximity of the lighter mass distributions.

We conclude that Cs experimental distributions when modified to predict the iodine distributions reproduce the neutron excessive part of our results and confirm that they correspond to the fission of target-like nuclei with an excitation energy of 20 ± 10 MeV in agreement with the quasielastic induced fission reaction concept. We note that the centroid of this distribution does not seem to move with the projectile energy. The cross sections increase until the energy reaches 250 MeV and then remain constant.

B. Complete fusion-fission component

We have seen that the main feature of the neutron deficient peak in the iodine mass distribution is the weak mass shift of the centroid with change in the projectile energy. Since our aim is to explain this behavior with a classical fusion-fission process, we have calculated these distributions based on a simple statistical model.

This model is a multi-step process in which three main sequential steps can be distinguished--first, compound nucleus formation; second, fission and third, deexcitation of the fission fragments. Since we must take into consideration the thick target nature of our experiments, in order to correlate our results with such calculations, we have to integrate the calculated results from the Coulomb barrier to the maximum energy of the beam. We have used 10 MeV steps in order to make this integration over the useful energy range.

The compound nucleus $^{278}(110)$ is produced with an energy in all cases larger than 40 MeV, thus the shell effects are negligible and as a consequence the calculation is based on the assumption that the fission barrier is close to zero. The competition between evaporation and fission, calculated using the "overlaid-ALICE"[15] code is found to completely favor fission and predicts that the number of neutrons emitted before fission is smaller than 0.3 and that the number of emitted charged particles is negligible.

The characteristics of the fission products are determined according to the model suggested by Reisdorf et al.[8] that is based on the Fong model[16] and assumes the minimum potential energy hypothesis for

two touching spheroids.

This model allows us to determine the most probable mass A_p' of the iodine fragment before deexcitation. Calculations[8] show that charge equilibration between the two touching fragments occurs more rapidly than mass equilibration. Thus for a given mass division the most probable charge division and spheroidal shapes for the two fragments were determined by minimization of the potential energy, W, with respect to the charge and shape parameters.

In order to calculate the variance σ_A^2 for the iodine isotopic distribution we used the following equations evaluated at the optimum charge for every possible mass division in the region of interest.

$$\sigma_A^2 = \sigma_z^2(A/Z)^2 \ . \qquad (2)$$

Here A and Z are for the fissioning nucleus and σ_z^2 was determined by the equation

$$\sigma_z^2 = T(2E_{pz})^{-1} \qquad (3)$$

where T is the nuclear temperature of the fissioning nucleus and E_{pz} is the parameter defined as

$$E_{pz} = \frac{1}{2}\left[\frac{\delta^2 W}{\delta Z^2}\right]_{Z=Z_p} \ . \qquad (4)$$

Again Z_p is the most probable value of Z found by minimization of the potential energy W. The calculated parameters A_p' and σ_A^2 are given in Table III.

The excitation energy of the two fragments E_F^* is given as follows:

$$E_F^* = E_{c.m.} - TKE + Q \qquad (5)$$

where $E_{c.m.}$ is the center-of-mass energy, TKE is the total kinetic energy of the fragments at infinity and Q is the energy balance of the reaction. The total kinetic energy is calculated using the semi-empirical formula given by Viola.[17]

$$TKE = \left[0.680 Z_1 Z_2 / A_1^{1/3} + A_2^{1/3}\right] + 22.2 \text{ MeV} . \qquad (6)$$

The excitation energy is assumed to be shared between the two fragments according to their mass ratio.

The deexcitation of the fragments is calculated with the "Overlaid-ALICE" evaporation code.[15] By not considering the angular momentum of the fragments, an error smaller than 0.3 amu in the final mass is introduced. Neutron evaporation is the most probable deexcitation mode, although for the highest energies proton emission must be taken into account. The calculation allows us to determine the average number, $\bar{\nu}_I$, of evaporated neutrons from the iodine fragment and the most probable mass of the fragment, A_p, after deexcitation. In order to know the width of the final isotopic distribution σ_t^2, we have $\sigma_t^2 = \sigma_A^2 + \delta_A^2$ where we have to add a small correction δ_A^2 to the calculated variance, σ_A^2, in order to account for the statistical fluctuations in the evaporation process and in the excitation energy resulting from the variance of the total kinetic energy of

the fragment. The correction is typically 0.9 amu. The resulting parameters are summarized in Table III.

Furthermore the final results take into account the enhanced proton emission for the neutron deficient nuclei and as a consequence the final distributions deviate slightly from a gaussian curve for the highest values of the energy.

The last step in the calculation is the integration of the calculated isotopic distribution over the energy range from the Coulomb barrier to the effective beam energy to get the distributions expected for a thick target. In order to do this we need to know the complete fusion cross section as a function of the projectile energy. We chose an average curve drawn through the available experimental points summarized by Kratz et al.[6] and shown in Fig. 3.

The semi-theoretical isotopic distributions calculated in this manner are drawn as solid lines in Fig. 2. The lines are drawn through our experimental points in order to show the agreement with the experimental data.

The agreement with the experimental data is good on the left side of the overall distribution and, particularly, the position of the centroid, A_p, of the CF/fission distribution is well-reproduced. The relatively small movement of the centroid with the energy is due, in first approximation, to the effect of the thickness of the target combined with the variation of the complete fusion cross section with energy and the increasing width of the iodine isotopic distributions with increasing energy.

C. Existence of a third fission component (DIT)

If we subtract the complete fusion-fission isotopic distribution (shown in Fig. 2 as a solid line) from the total overall isotopic distribution (shown as a dot dashed line) the resulting distribution (dashed line plus dotted line) is non-gaussian in shape and has a shoulder in the mass 130 region to the gaussian isotopic distribution resulting from QET induced fission. Thus it appears that there is an enhancement of yields in the iodine isotopic distribution around mass A = 130, that can not be accounted for by QET or CF induced fission reactions. We may attribute this phenomenon to fission following deep inelastic transfer (DIT) reactions. These enhanced yields come from the fission of uranium-like nuclei produced in DIT reactions, which have a higher excitation energy than those produced in QET reactions. The high excitation energy results in more neutron deficient iodine products. However, since there is a continuous trend in excitation energy and mass transfer between the QET and DIT reactions it is not possible to make a meaningful separation into distinct distributions for each mechanism. Thus the neutron rich iodine distribution should be regarded as being composed of primarily a gaussian QET induced fission distribution with some deviation from a gaussian shape (in the mass region from 128 to 132) due to DIT induced fission production of iodine isotopes.

IV. TRENDS OF THE CROSS SECTIONS AS A FUNCTION OF ENERGY

A. Relative strengths of the QET, DIT and CF reactions

Figure 2 shows that the production cross sections for iodine isotopes from QET induced fission and CF induced fission have a different behavior at the energies close to the Coulomb barrier, the value of which is 200 MeV (r_o = 1.44 fm) in the laboratory system.[1,7] Figure 4 shows a plot of the ratio of the integrated cross section for the production of iodine isotopes from fission following CF to that from fission following QET. The drastic change in slope of the curve shows that the cross section for QET is a relatively predominant fraction of the total cross section near the Coulomb barrier and decreases in relative importance at higher energy.

If we assume that the overall fission mass distribution remains symmetric and peaked near half the mass of the compound nucleus, then the trends in the iodine isotopic distributions reflect the trends in the identified reaction mechanisms and there is a higher threshold for the complete fusion than for the quasielastic transfer (and deep inelastic transfer) reaction.

Alternatively, if the mass distribution associated with fission of the compound nucleus became asymmetric near the barrier the ratio shown in Fig. 4 would not reflect the differences in the thresholds for the CF and QET reaction since the iodine yields from complete fusion would correspond to a nearly symmetric division and therefore would have relatively small fission yields. Kalpakchieva et al.[18] have suggested that such an effect occurs for excitation energies

$E^* \leq 50$ MeV in the $^{40}Ar + ^{243}Am$ reaction.

Kalpakchieva et al.[18] have studied the mass distribution from the reaction of ^{40}Ar with ^{243}Am at several compound nucleus, $^{283}(113)$, excitation energies. At the lower excitation energies ($E^* \leq 50$ MeV) they find the mass distribution to be very asymmetric with one peak in the lead region ($200 \leq A \leq 210$). The products they observe are selected by kinematic analysis to be associated with full momentum transfer events. Thus, arguments are presented that the asymmetric mass distributions correspond to the fission of the compound nucleus and results from stablizing shell effects in the doubly magic ^{208}Pb region. Central to this point of view is the angular distribution of the fission products. The angular distribution results of Kalpakchieva et al.[18] appear to be symmetric about 90^o in the c.m. system. However, based on a method developed by Otto et al.,[13] preliminary recoil range measurements[19] of products from Hf to Bi for the reaction of $^{40}Ar + ^{238}U$ and $^{48}Ca + ^{238}U$ (at excitation energies between 50 and 80 MeV) indicate that the corresponding angular distributions are not symmetric about 90^o but are peaked at backward angles thus suggesting the deep inelastic transfer reaction.

It is our view that the results of Kalpakchieva et al.[18] correspond to the observation of deep inelastic transfer reactions at the lower excitation energies where an asymmetric mass distribution is observed. This view is based on 1) the inferred deep inelastic type angular distributions for products in the Hf to Bi region,[19] for the $^{40}Ar + ^{238}U$ reaction, CN = $^{278}(110)$, and for the $^{48}Ca + ^{238}U$ reaction, CN = $^{286}(112)$, and 2) the fact that we may interpret the

$^{40}Ar + ^{243}Am$ results in an alternative way consistent with a higher threshold for complete fusion as follows. For the lower excitation energies the higher mass peak of the observed asymmetric mass distribution corresponds only to a deep inelastic transfer reaction mass distribution, since no complete fusion is occurring. At the higher excitation energies the threshold for complete fusion is exceeded and a symmetric mass distribution[18] is observed as expected.

Thus we believe the ratio of iodine yields from the identified reaction mechanisms reflects the relative differences in the threshold energies for these mechanisms. Our data may then be interpreted as evidence for a higher threshold energy for the complete fusion reaction than for the quasielastic transfer or deep inelastic transfer reactions. In agreement with our results, it was noticed by Videbeck et al.,[20] for the $^{16}O + ^{208}Pb$ reaction that most of the reaction cross section is associated with QET near the Coulomb barrier and that the QET reaction is less important at higher energies. The onset of QET reactions at energies (10 to 15 MeV) below the CF threshold was also observed by Nitschke et al.,[21] for the reaction of ^{40}Ar and ^{208}Pb but they found no difference in thresholds for the reaction of ^{48}Ca and ^{208}Pb. Oganessian et al.[22] observed a 30 MeV difference between the transfer reaction threshold and fission threshold in the reaction of ^{74}Ge and ^{232}Th although Oganessian et al.[23] report no difference for the reaction of ^{40}Ar and ^{208}Pb and the reaction of ^{40}Ar and ^{238}U. Lefort[24] also reported on even larger difference for the transfer and quasi-fission reaction of ^{84}Kr with ^{238}U, in agreement with predictions that the effect should be larger with heavier projectiles. A difference in

threshold is just what may be expected since a transition from the less penetrating surface reactions to more penetrating overlap of the target and projectile occurs as the energy increases. Bass[25,26] has identified the "interaction barrier" for quasielastic nuclear reactions as the energy required to bring the target and projectile to within range of their mutual nuclear forces for a head-on collision. He points out that at this interaction separation distance the resultant Coulomb plus nuclear forces are still repulsive. The fusion threshold is then defined for a zero angular momentum collision as the maximum value of the potential barrier where the Coulomb and nuclear forces just balance.

B. Threshold for complete fusion

The probability of producing superheavy elements is directly related to the threshold for complete fusion in heavy-ion reactions with heavy targets such as ^{208}Pb, ^{238}U and ^{248}Cm, since the minimum excitation energy is desired in such reactions. As a result much theoretical effort has been directed to understanding the dynamics of compound nucleus formation in heavy-ion reactions.[25-29] There has been somewhat less experimental work[1,7] done on the reaction of $^{40}Ar + ^{238}U$.

Sikkeland[1] reported the excitation function for the $^{40}Ar + ^{238}U$ reaction. The barrier for this reaction is 171 MeV (c.m.). Since QET, DIT and CF induced fission are all included in this excitation function Bass[25,26] has taken this threshold to be the interaction barrier.

Oganessian et al.[7] have measured the excitation function of gold

products from the $^{40}Ar + ^{238}U$ reaction and also obtained a reaction threshold of 171 MeV (c.m.). Based on the range distribution measurements of Otto et al.[19] for Au products in the same reaction we believe these products may be formed primarily in deep inelastic transfer reactions. This value, however, is in agreement with the results of Sikkeland[1] and consistent with the assumption that 200 MeV (lab) is the interaction barrier for quasielectric transfer and close to that for deep inelastic transfer reactions.

Our objective is to estimate the relative difference between the complete fusion threshold and the interaction barrier by using the ratios shown in Fig. 4. To do this, the excitation function for the total reaction cross section must be known and used. Due to the small number of cross-section data that we have obtained in the barrier region we choose to take the excitation function of Sikkeland[1] as representative of the total reaction cross section. This excitation function can be relatively well estimated with the easily integrated function given in Eq. (7), using the value of r_o = 1.44 fm, as suggested by Oganessian,[7] to obtain B = 171 MeV (c.m.) and R = 13.85 fm.

$$\sigma_R = \pi R^2 \left(1 - \frac{B}{E}\right) . \qquad (7)$$

The iodine cross sections measured in these thick target experiments represent average cross sections over the energy region from the incident energy to the Coulomb barrier. Therefore, the measured ratios σ_{CF}/σ_{QET} should be applied to the average total reaction cross section, $\bar{\sigma}_R$, where

$$\bar{\sigma}_R = \frac{1}{E-B} \int_B^E \sigma_R \, dE = \pi R^2 \left(1 - \frac{B}{E-B} \ln \frac{E}{B}\right) . \quad (8)$$

An effective bombarding energy (E_{eff}) can be defined in the following way:

$$\bar{\sigma}_R = \pi R^2 (1-B/E_{eff}) . \quad (9)$$

As shown in Fig. 5 a plot of $\bar{\sigma}_R$ vs $1/E_{eff}$ produces a straight line with an intercept equal to 1/B. The effective bombarding energy can be calculated for any thick target experiment by equating Eqs. (8) and (9) and solving for E_{eff} to obtain

$$E_{eff} = (E-B)/\ln(E/B) . \quad (10)$$

First approximations for the relative average complete fusion cross section ($\bar{\sigma}_{CF}$) were obtained as the product of $\bar{\sigma}_R$ and $[(\sigma_{QET}/\sigma_{CF}) + 1]^{-1}$ and plotted against E_{eff}^{-1}. A threshold for complete fusion was obtained, but as can be seen from Eq. (10) the effective bombarding energies must be recalculated, as must the cross sections for the complete fusion products since a higher barrier implies a shorter range to the barrier and a smaller number of target atoms. These corrections have been made and the final $\bar{\sigma}_{CF}$ vs E_{eff}^{-1} is plotted in Fig. 5. A least-squares fit to the four data points corresponding to the incident bombarding energies of 240, 250, 270, and 290 MeV (Lab) gives an intercept corresponding to a barrier of 183 MeV (c.m.), which is 12 MeV higher than the interaction barrier. Extrapolation of the dashed line (Fig. 5) through the upper limit for $\bar{\sigma}_{CF}$ corresponding to the incident bombarding energy of 226 MeV (Lab) suggests that the

barrier is actually equal to or greater than 186 MeV (c.m.) and that the relative difference between the complete fusion threshold and the interaction barrier is equal to or greater than 15 MeV (c.m.). Since the variations of the width of the complete fusion mass distribution are not well known and expected to have only a small effect[7] on the ratio σ_{CF}/σ_{QET}, they were not used in the calculation. However inclusion of this variation would further reduce the relative complete fusion cross section in the threshold region resulting in an even higher estimate of the threshold energy. The dot dashed line, drawn to pass through the point corresponding to 340 MeV, in Fig. 5 indicates that the complete fusion cross section does not continue to increase in geometric proportion with $\bar{\sigma}_R$. Such an effect could be correlated with a critical angular momentum. Kratz et al.[6] discuss the relationship between the critical angular momentum and the complete fusion cross section for the $^{40}Ar + ^{238}U$ system in the light of several models. However the lack of experimental data above 340 MeV in this work does not justify drawing conclusions concerning the relationship of a critical angular momentum and the complete fusion cross section.

The excitation functions shown in Fig. 5 are replotted in Fig. 6. These excitation functions as shown with $\bar{\sigma}$ vs. E_{eff} can be directly compared with future excitation functions plotted as $d\sigma/dE$ vs $E_{(c.m.)}$ obtained for this reaction using thin targets. The results of this work suggest that such a careful study of the interaction excitation function and the complete fusion threshold should be made.

The threshold for complete fusion appears to be greater than 186 MeV (c.m); thus we conclude that the complete fusion threshold is at least 15 MeV (c.m.) higher than the interaction barrier. Bass[25,26] has calculated the interaction threshold and the fusion threshold for the reaction of ^{40}Ar and ^{238}U. He obtained 177 MeV (c.m.) for the quasielastic transfer barrier and 190 MeV (c.m.) for the fusion barrier. Thus Bass would predict the fusion threshold to be 13 MeV (c.m.) higher than the interaction barrier.

Calculations of the fusion barrier have also been made using the proximity force theorem as suggested by Blocki et al.[29] Using the parameters suggested we calculated the fusion threshold to be 180 MeV (c.m.) that is 9 MeV (c.m.) higher than 171 MeV (c.m.), the interaction barrier. Since both of these theoretical calculations are in agreement with our results we conclude that the inclusion of a finite range for the mutual nuclear forces between two heavy nuclei properly predicts higher complete fusion thresholds for heavy-ion reactions with uranium-like targets where the projectile mass is approximately equal to 40.

Using the proximity force model we calculate the threshold energy for fusion in the $^{48}Ca + ^{248}Cm$ reaction to be 203 MeV (c.m.). The interaction barrier (using $r_o = 1.44$) would be 193 MeV (c.m.). Using the Bass model we get 212 MeV (c.m.) for the complete fusion threshold and 198 MeV (c.m.) for the interaction barrier. The effect of this higher threshold for complete fusion would be to raise the minimum excitation energy achievable for the superheavy element compound nucleus $^{296}(116)$ and greatly reduce the chances for observing superheavy elements in their ground state, consistent with negative experimental results.[30,31]

V. SUMMARY

The measurement of iodine isotopic distributions in the reaction $^{40}Ar + ^{238}U$ at different projectile energies shows the existence of three reaction components corresponding to three different processes:

1. Quasielastic transfer (QET),
2. Deep inelastic transfer (DIT),
3. Complete fusion (CF),

followed by fission of the heavy-reaction product.

The observed unexpected stable position of the centroid of the complete fusion induced fission distribution is found to be in agreement with calculations based on the statistical model for fission and on evaporation calculations with the "overlaid-ALICE" code. Important for this observation is the integral nature of the thick target experimental method.

The ratios of the cross sections for complete fusion and quasielastic transfer processes indicate that the threshold for the fusion reaction is higher than for the quasielastic transfer reaction and this threshold appears to be above the interaction barrier for QET and DIT reactions. An observed experimental difference of greater than 15 MeV (c.m.) between the fusion threshold and the interaction barrier can be compared with theoretical calculations using the models suggested by Bass[25,26] and Blocki[29] that predict 13 MeV and 9 MeV, respectively. Such an effect reduces the chances of making SHE's in reactions such as $^{48}Ca + ^{248}Cm$ assuming the same enhancement of threshold exists since the additional excitation energy enhances the losses due to fission.

ACKNOWLEDGMENTS

The author would like to express their appreciation to Mrs. D. Lee, Dr. I. Binder and Mr. D. Morrissey for their help and assistance. The participation of Dr. Malcolm Fowler in the experimental aspects of this work is gratefully acknowledged. We would like to thank Mr. D. Morrissey for providing the results of his calculations of the fusion thresholds using the Bass model and the proximity force model and Dr. W. D. Loveland for some helpful comments and suggestions. One of us (M.S.S.) is happy to acknowledge the hospitality and financial support of the Nuclear Science Division of the Lawrence Berkeley Laboratory. The experiments were carried out at the SuperHILAC facility of the Lawrence Berkeley Laboratory. This work was supported in part by the High Energy and Nuclear Physics Division of the U. S. Department of Energy.

REFERENCES

1. T. Sikkeland, Ark. Fys. 36, 539 (1967); Phys. Lett. 27B, 277 (1968).
2. F. Hanappe, C. Ngo, J. Peter and B. Tamain, in Proceedings of the Third Symposium on the Physics and Chemistry of Fission, Rochester (1973).
3. A. G. Arthuk, G. F. Gridnev, V. L. Mikheev, V. V. Volkov, and J. Wilcynski, Nucl. Phys. A215, 91 (1973).
4. Nguyen Tac Anh, Y. T. Oganessian, and Y. E. Penionzhkevich, in Proceedings of the International Conference on Reactions Between Complex Nuclei, Nashville, June 1974.
5. A. G. Arthuk, G. F. Gridnev, V. L. Mikheev, and V. V. Volkov, JINR E7-8590, 1975.
6. J. V. Kratz, J. O. Liljenzin, A. E. Norris, and G. T. Seaborg, Phys. Rev. C 13, 1347 (1976).
7. Yu. Ts. Oganessian, Yu. E. Penionzhkevich, K. A. Gavrilov and Kim DeEn, Sov. J. Nucl. Phys. 21, 126 (1975).
8. W. Reisdorf, M. de Saint-Simon, L. Remsberg, L. Lessard, C. Thibault, E. Roechkl, and R. Klapisch, Phys. Rev. C 14, 2189 (1976).
9. L. C. Northcliffe and R. F. Schilling, Nucl. Data Tables A7, 233 (1970).
10. M. M. Fowler, D. Lee, R. J. Otto, and I. Binder, Lawrence Berkeley Laboratory Report, LBL-4000 (1974), p. 395.
11. I. Binder, J. V. Kratz, J. O. Liljenzin, A. E. Norris and G. T. Seaborg, Lawrence Berkeley Laboratory Report, LBL-2366, (1973) p. 61.

12. B. L. Tracy, J. Chaumont, R. Klapisch, J. M. Nitschke, A. M. Poskanzer, E. Roeckl, and C. Thibault, Phys. Rev. C 5, 222 (1972).

13. R. Otto, M. Fowler and G. T. Seaborg, to be published in Phys. Rev. C (1978).

14. J. V. Kratz, A. E. Norris and G. T. Seaborg, Phys. Rev. Lett. 33, 502 (1974).

15. M. Blann, COO-3494-29; M. Blann and F. Plasil, Phys. Rev. Lett. 29, 303 (1972); F. Plasil and M. Blann, Phys. Rev. C 11, 508 (1975); COO 3494-32, "Overlaid ALICE, Description, Revisions."

16. P. Fong, Phys. Rev. 102, 434 (1956).

17. V. E. Viola, Jr., Nucl. Data 1, 391 (1966).

18. R. Kalpakchieva, Y. T. Oganessian, Y. E. Penionzhkevich, M. Sodan, Z. Physik A283, 253 (1977).

19. R. J. Otto, D. J. Morrissey, W. Loveland, and G. T. Seaborg, Lawrence Berkeley Laboratory Report LBL-7188, submitted to Z. Physik A.

20. F. Videbeck, R. B. Goldstein, L. Grodzins, S. G. Steadman, T. A. Belote, J. D. Garett, Phys. Rev. C 15, 954 (1977).

21. J. M. Nitschke, R. E. Leber, M. J. Nurmia and A. Ghiorso, Lawrence Berkeley Laboratory Report LBL-6534 Rev. 8 (1978).

22. Yu. Ts. Oganessian, D. M. Nadkarin, Nguen TakAn, Yu. E. Penionzhkevich, and B. I. Pustyl'nik, Yad Fiz 9, 715 (1969) [Sov. J. Nucl. Phys. 9, 414 (1970)].

23. Yu. Ts Oganessian and Yu. E. Penionzhkevich, JINR E7-9187 (1975).

24. M. Lefort, C. Ngo, J. Peter and B. Tamain, Nucl. Phys. A216, 166 (1973).

25. R. Bass, Nucl. Phys. A231, 45 (1974).

26. R. Bass, Phys. Lett. 47B, 139 (1973).

27. V. D. Toneev and R. Schmidt, JINR P7-10452 (1977).

28. C. F. Tsang, Lawrence Berkeley Laboratory Report LBL-2366, (1973), p. 146.

29. J. Blocki, J. Randrup, W. J. Swiatecki and C. F. Tsang, Ann. Phys. 105, 427 (1977).

30. E. K. Hulet, R. W. Lougheed, J. F. Wild, J. H. Landrum, P. C. Stevenson, A. Ghiorso, J. M. Nitschke, R. J. Otto, D. J. Morrissey, P. A. Baisden, B. F. Gavin, D. Lee, R. J. Silva, M. M. Fowler, and G. T. Seaborg, Phys. Rev. Lett. 39, 385 (1977).

31. R. J. Otto, D. J. Morrissey, D. Lee, A. Ghiorso, J. M. Nitschke G. T. Seaborg, M. M. Fowler and R. J. Silva, to be published in J. Inorg. Nucl. Chem. (1978).

Table I. Summary of ^{40}Ar + ^{238}U irradiations.

Incident[a] Energy (MeV)	Average Beam Flux (particles/sec)	Length of Bombardment (min)	Effective[b] Target Thickness (mg/cm^2)	Chemical Yield (%)
212±3	2.2×10^{11}	212	1.0	41±1
226±3	3.9×10^{11}	80	3.0	41±1
240±3	2.0×10^{11}	75	6.0	42±1
250±3	1.9×10^{11}	83	8.0	38±1
270±3	4.1×10^{11}	108	11.0	37±1
290±3	1.5×10^{11}	63	15.5	39±1
340±5	--[c]	161	26.0	50±5

[a]Corrections have been made for Al cover layer on the target and the energy defect in the surface barrier detector.
[b]Based on B_{lab} = 200 MeV.
[c]Absolute intensity unknown.

Table II. Independent yield cross sections (mb) for iodine isotopes from the $^{40}Ar + ^{238}U$ reaction.

Mass Number	E_{lab} = 212 MeV	E_{lab} = 226 MeV	E_{lab} = 240 MeV	E_{lab} = 250 MeV	E_{lab} = 270 MeV	E_{lab} = 290 MeV	Cross Sections (arbitrary units) E_{lab} = 340 MeV
121					0.904±0.009		0.357±0.019
123			0.294±0.003	0.541±0.027	0.791±0.008	1.54±0.02	1.58±0.079
124[a]			0.683±0.028	1.241±0.287	1.65±0.19	3.00± 0.23	2.64±0.13
126[a]			2.340±0.069	3.545±0.045	4.34±0.24	7.17±0.07	5.64±0.58
128[a]				3.118±0.031	3.77±0.038	5.51±0.06	4.52±0.22
130[a]	0.184±0.004	0.952±0.064	2.29±0.15	3.214±0.098	3.65±0.16	5.39±0.17	4.55±0.28
131	0.305±0.005	1.011±0.011	1.802±0.20	2.540±0.042	2.95±0.03	3.39±0.10	2.85±0.20
132	0.500±0.030	1.327±0.013	2.92±0.31	4.791±0.229	3.25±0.28	5.83±0.48	3.62±0.50
133	1.124±0.028	3.586±0.036	6.28±1.20	7.876±0.005	8.23±0.36	8.96±0.19	8.54±0.47
134	1.449±0.028	4.466±0.092	8.12±0.15	9.582±0.161	9.88±0.14	9.47±0.12	11.06±0.56
135	1.454±0.027	4.680±0.064	8.12±0.10	10.05±0.14	9.20±0.15	10.68±0.15	8.00±0.41

[a]Measured independent yields.

Table III. Calculated parameters for iodine isotopic distributions.

E_{lab} (MeV)	A_p' [a]	E*(MeV)	$\bar{\nu}_I$ [b]	A_p [c]	σ_A^2 [d]	σ_t^2 [e]
212	133.8	66.2	6.5	127.3	3.13	3.93
226	133.8	74.4	7.1	126.7	3.70	4.50
240	133.8	78.6	7.5	126.3	3.93	4.76
250	133.8	82.7	7.6	126.2	4.15	4.95
270	133.8	86.8	7.8	126.0	4.60	5.40
290	133.8	99.2	8.2	125.6	4.98	5.78
340	133.8	119.8	8.9	124.9	5.88	6.68

[a] Most probable mass of the iodine fragment before deexcitation.
[b] Number of evaporated neutrons from A_p'.
[c] Most probable mass of the iodine fragment after deexcitation.
[d] Isotopic distribution variance of the fission process.
[e] Total isotopic distribution variance after the deexcitation.

FIGURE CAPTIONS

Fig. 1. Production cross sections for the measured partial cumulative and independent iodine yields from the reaction of ^{40}Ar with thick ^{238}U targets. The incident energy of the ^{40}Ar beam is shown with each corresponding set of data (connected by dashed lines).

Fig. 2. Independent yield cross sections for the production of iodine isotopes in the thick target reaction of ^{40}Ar with ^{238}U. The solid lines, dashed lines, dot-dashed lines and dotted lines are explained in the text.

Fig. 3. Measured complete fusion cross sections based on experimental data compiled by Kratz et al.[6] The solid line was used to integrate the theoretical iodine isotopic distributions from the Coulomb barrier to the effective beam energy.

Fig. 4. The ratio (expressed as percent) of the cross section for the production of iodine isotopes by complete fusion-fission (σ_{CF}) and by quasielastic transfer induced fission (σ_{QET}) in the thick target reaction of ^{40}Ar with ^{238}U. The solid line is drawn to pass through the data points.

Fig. 5. A plot of $\bar{\sigma}_R$ and $\bar{\sigma}_{CF}$ vs E_{eff}^{-1} where $\bar{\sigma}_R$ is the average total reaction cross section calculated by using the parameters indicated and $\bar{\sigma}_{CF}$ is the average complete fusion cross section. See text for further explanation of the effective bombarding energy, E_{eff}, and the solid, dashed and dot-dashed lines.

Fig. 6. A plot of $\bar{\sigma}_{CF}$ and $\bar{\sigma}_R$ vs the effective bombarding energy, E_{eff}. The solid lines, dashed and dot-dashed lines correspond to the same lines shown in Fig. 5. See text for further explanation.

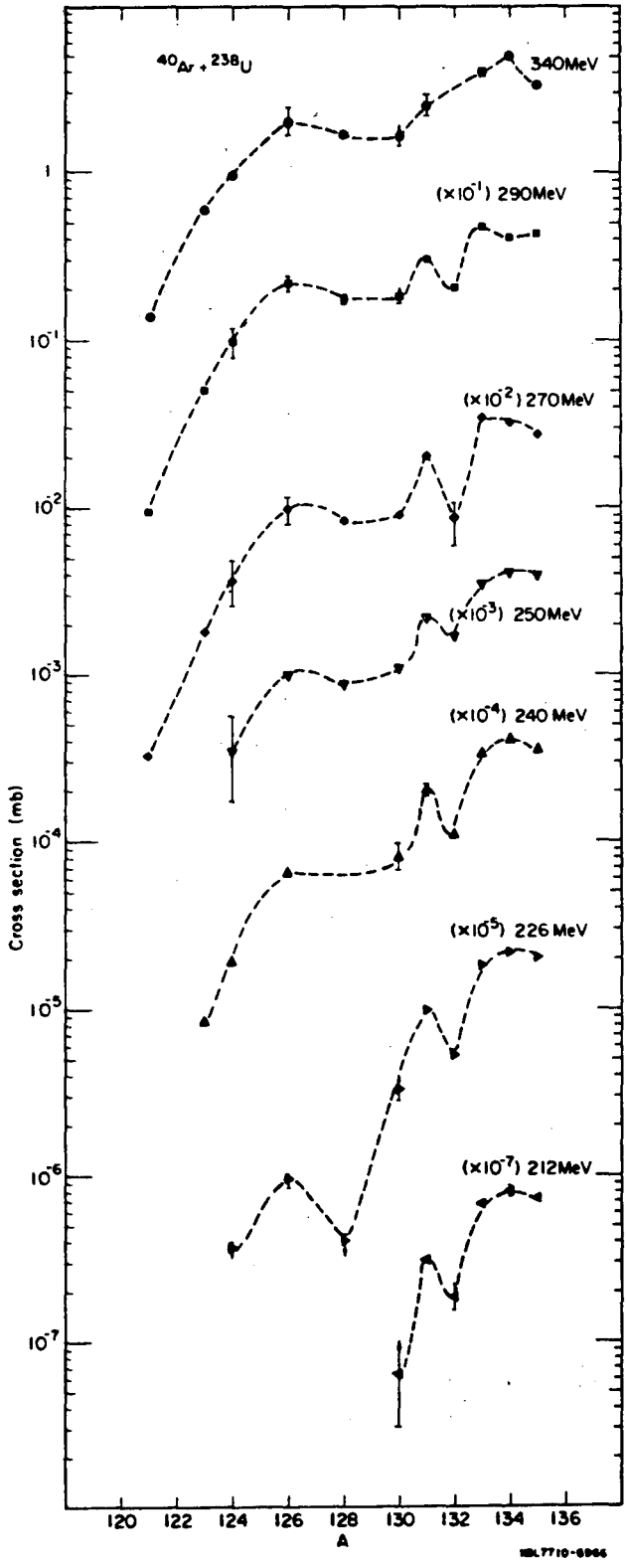

Fig. 1

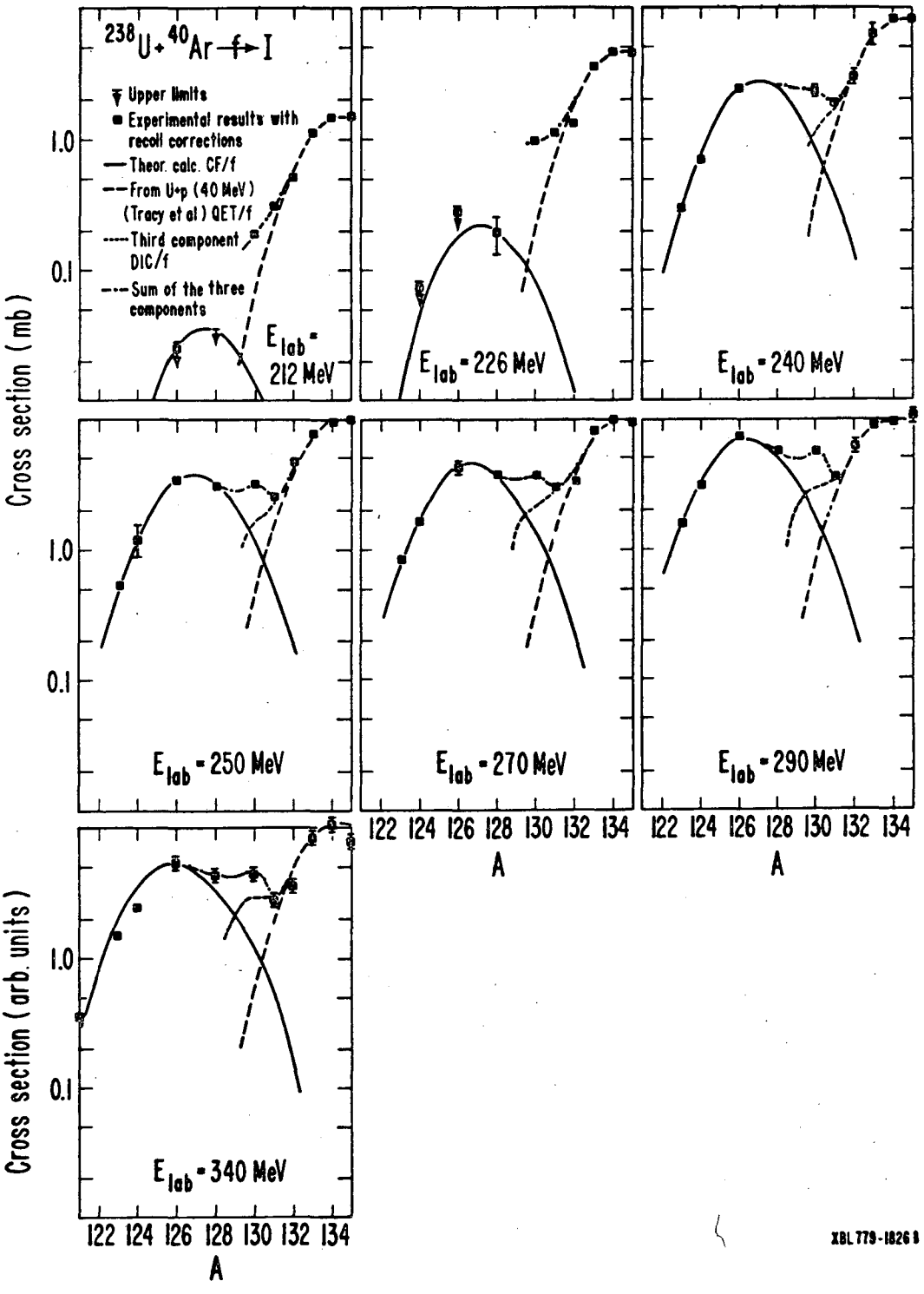
$^{238}U + ^{40}Ar \rightarrow f \rightarrow I$
Upper limits
Experimental results with recoil corrections
Theor. calc. CF/f
From U+p (40 MeV) (Tracy et al) QET/f
Third component DIC/f
Sum of the three components
E_{lab} = 212 MeV
E_{lab} = 226 MeV
E_{lab} = 240 MeV
E_{lab} = 250 MeV
E_{lab} = 270 MeV
E_{lab} = 290 MeV
E_{lab} = 340 MeV
Cross section (mb)
Cross section (arb. units)
1.0
0.1
122 124 126 128 130 132 134
A
XBL 779-1826 B

Fig. 2

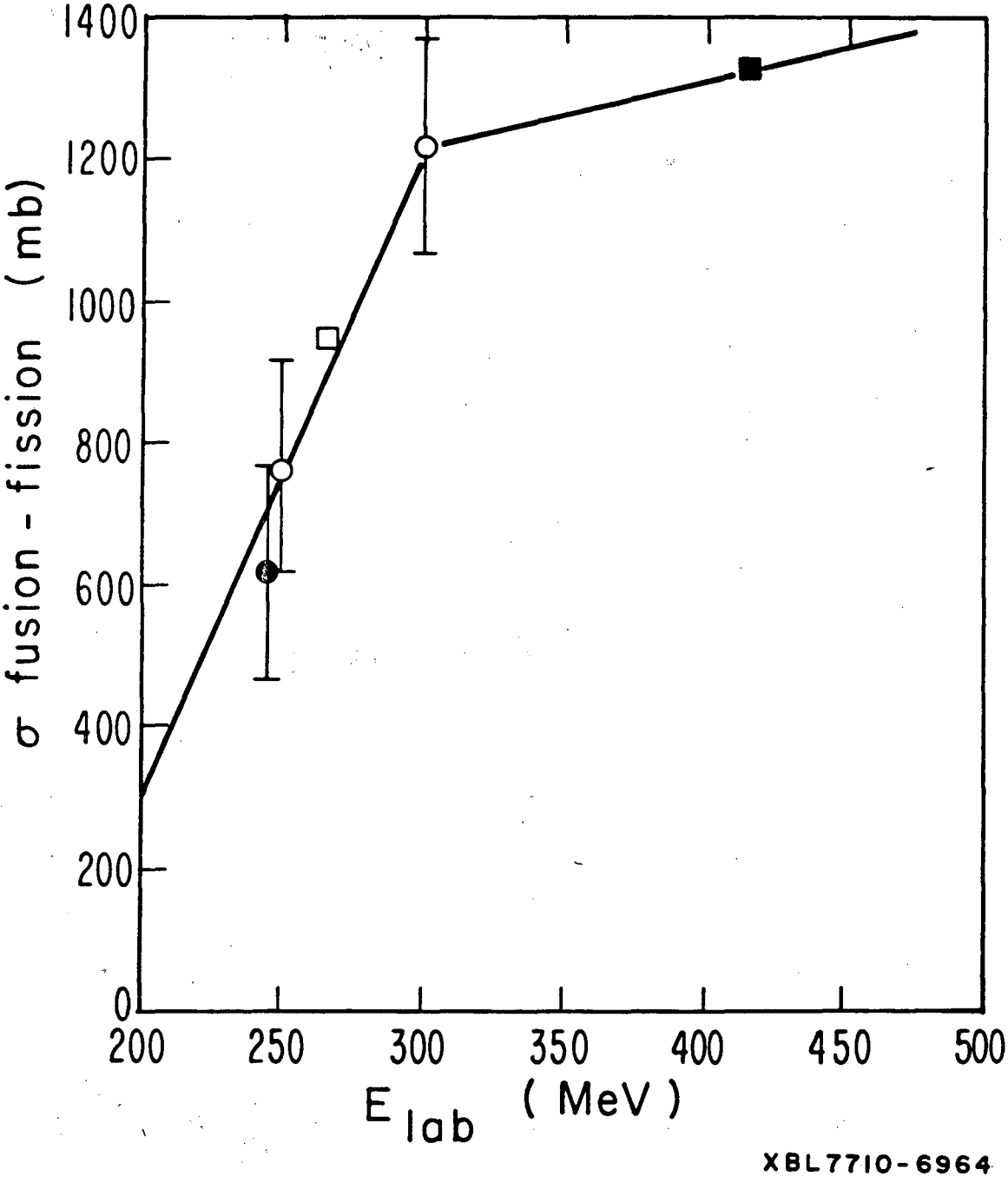

Fig. 3

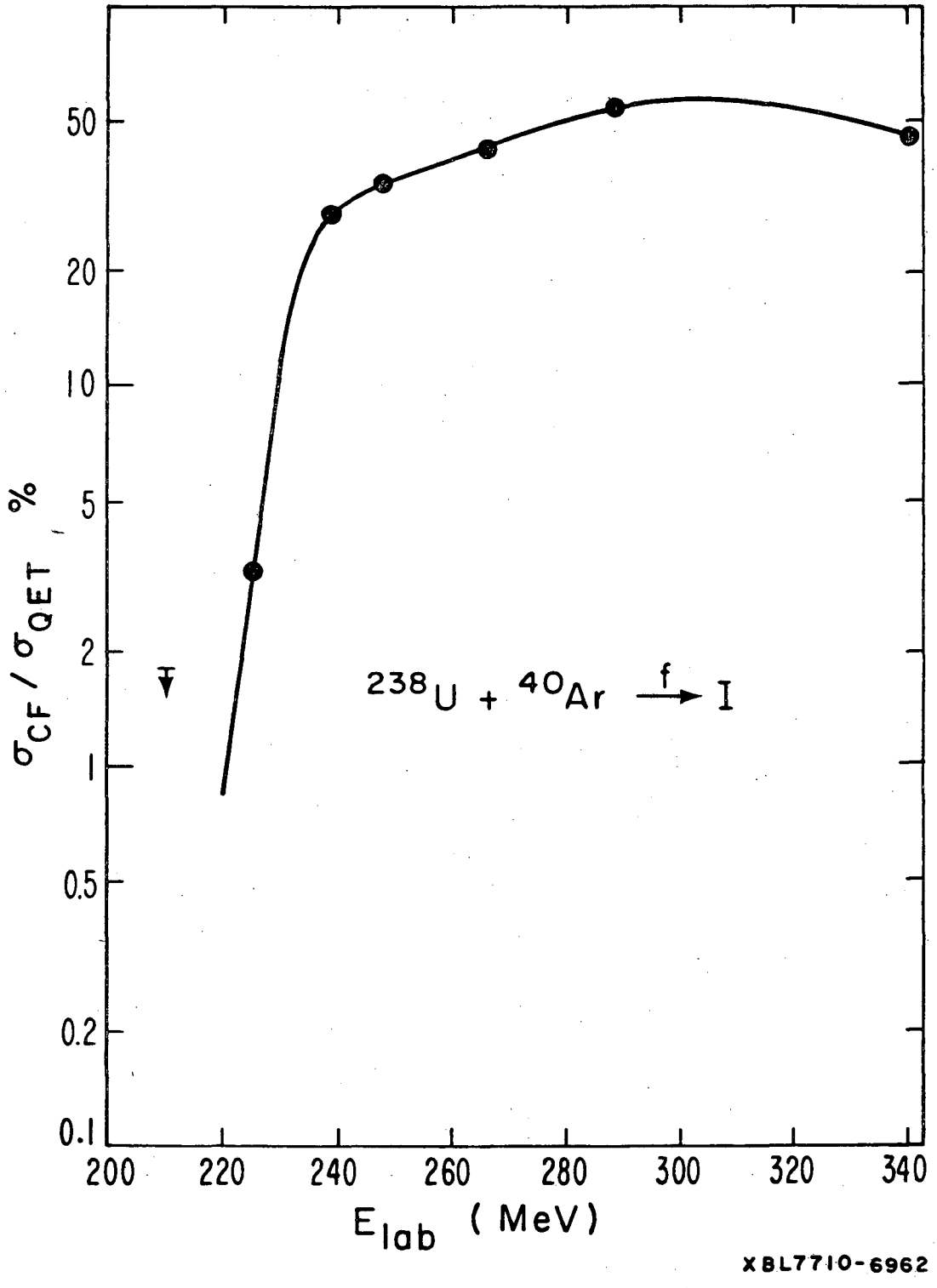
50
20
10
5
2
1
0.5
0.2
0.1
$\sigma_{CF} / \sigma_{QET}$ %
$^{238}U + ^{40}Ar \xrightarrow{f} I$
200
220
240
260
280
300
320
340
E_{lab} (MeV)
XBL7710-6962

Fig. 4

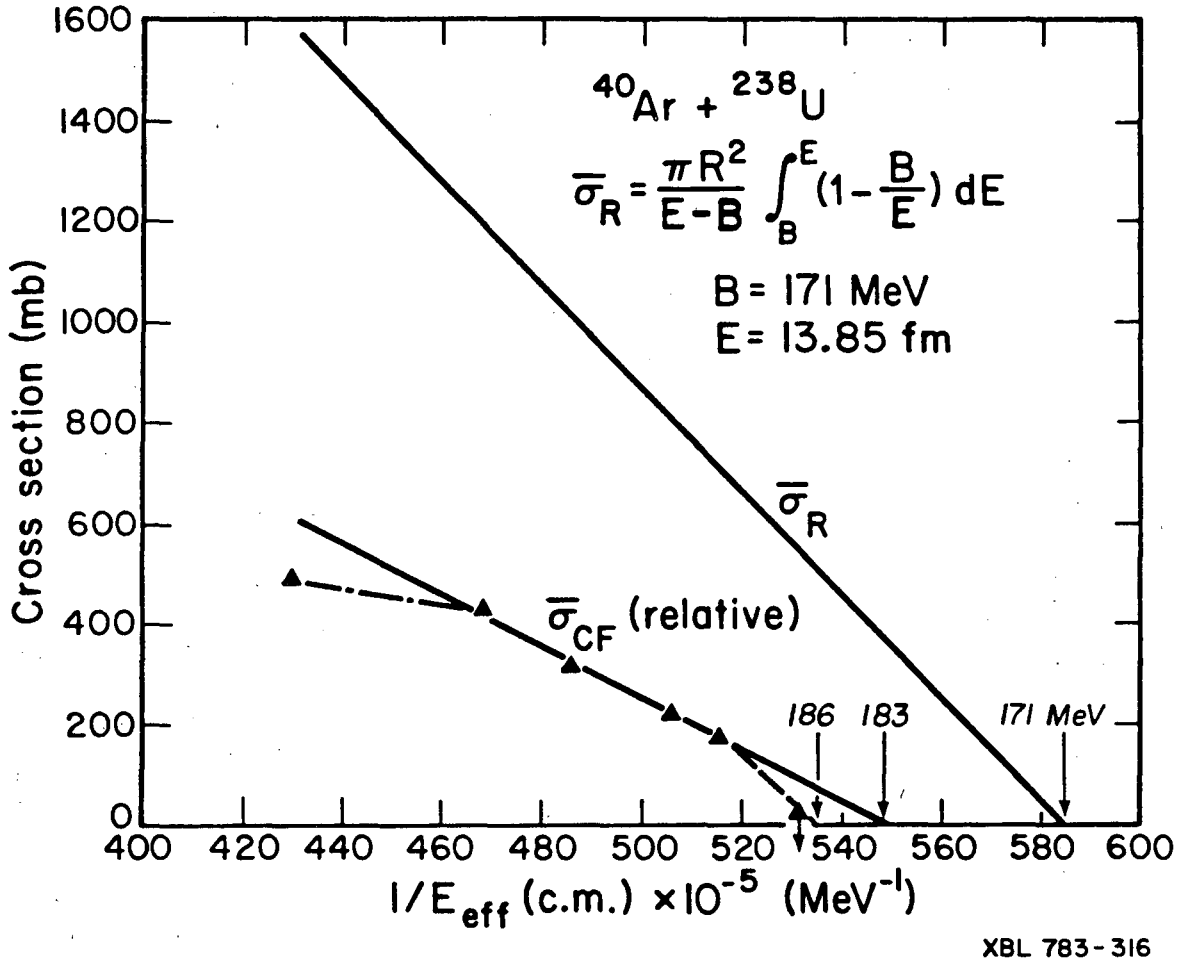

Fig. 5

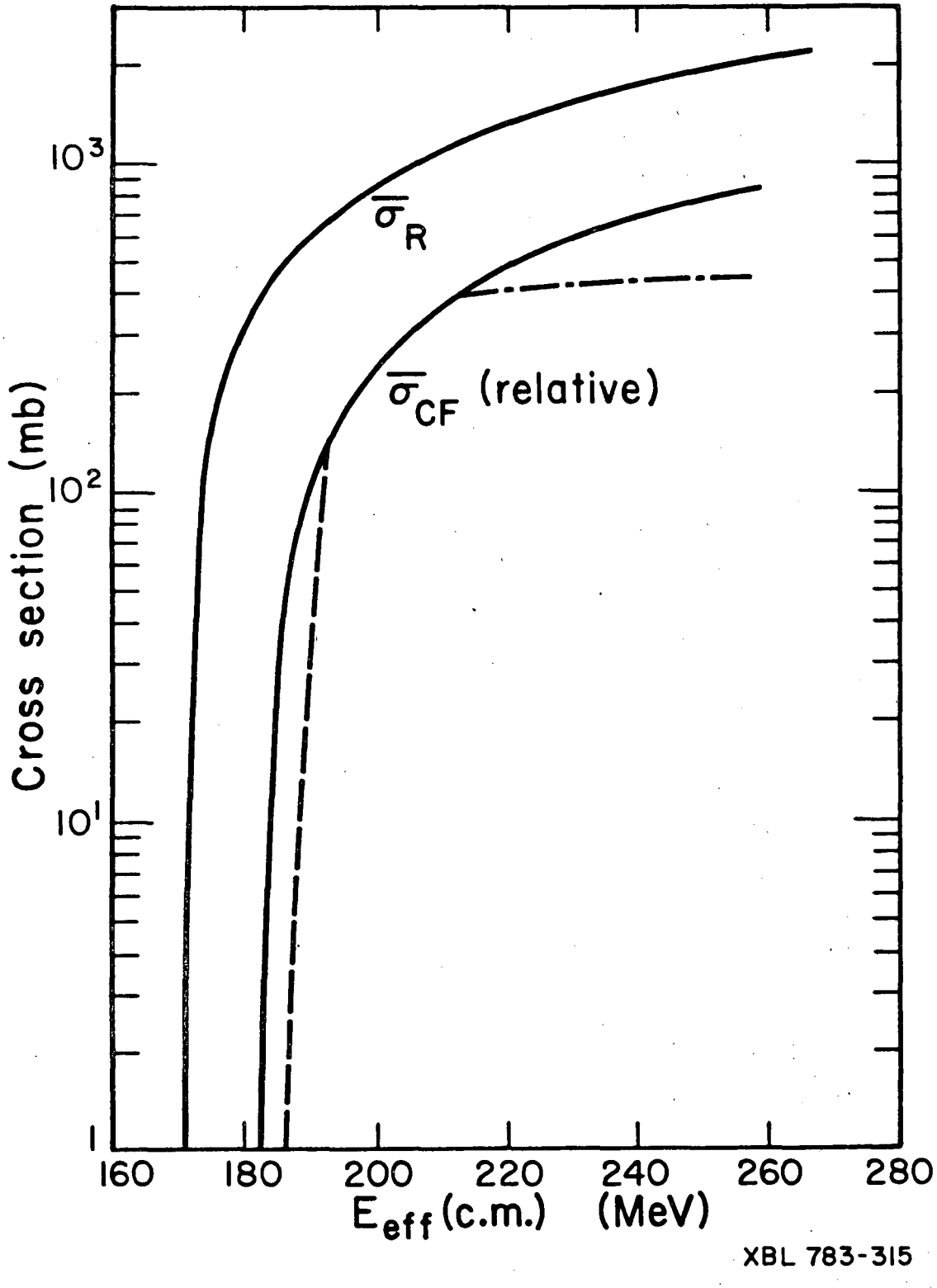
10^3
10^2
10^1
1
Cross section (mb)
$\overline{\sigma}_R$
$\overline{\sigma}_{CF}$ (relative)
160
180
200
220
240
260
280
E_{eff} (c.m.) (MeV)
XBL 783-315

Fig. 6

TECHNICAL INFORMATION DEPARTMENT
LAWRENCE BERKELEY LABORATORY
UNIVERSITY OF CALIFORNIA
BERKELEY, CALIFORNIA 94720